Journal of Biomedical Optics

BiomedicalOptics.SPIEDigitalLibrary.org

Mapping of hemoglobin in erythrocytes and erythrocyte ghosts using two photon excitation fluorescence microscopy

Katarina Bukara
Svetlana Jovanić
Ivana T. Drvenica
Ana Stančić
Vesna Ilić
Mihailo D. Rabasović
Dejan Pantelić
Branislav Jelenković
Branko Bugarski
Aleksandar J. Krmpot

SPIE.

Katarina Bukara, Svetlana Jovanić, Ivana T. Drvenica, Ana Stančić, Vesna Ilić, Mihailo D. Rabasović, Dejan Pantelić, Branislav Jelenković, Branko Bugarski, Aleksandar J. Krmpot, "Mapping of hemoglobin in erythrocytes and erythrocyte ghosts using two photon excitation fluorescence microscopy," *J. Biomed. Opt.* **22**(2), 026003 (2017), doi: 10.1117/1.JBO.22.2.026003.

Mapping of hemoglobin in erythrocytes and erythrocyte ghosts using two photon excitation fluorescence microscopy

Katarina Bukara,[a] Svetlana Jovanić,[b] Ivana T. Drvenica,[a,c] Ana Stančić,[c] Vesna Ilić,[c] Mihailo D. Rabasović,[b] Dejan Pantelić,[b] Branislav Jelenković,[b] Branko Bugarski,[a] and Aleksandar J. Krmpot[b,d,*]
[a]University of Belgrade, Department of Chemical Engineering, Faculty of Technology and Metallurgy, Belgrade, Serbia
[b]University of Belgrade, Institute of Physics Belgrade, Belgrade, Serbia
[c]University of Belgrade, Institute for Medical Research, Belgrade, Serbia
[d]Texas A&M University at Qatar, Science Program, Doha, Qatar

Abstract. The present study describes utilization of two photon excitation fluorescence (2PE) microscopy for visualization of the hemoglobin in human and porcine erythrocytes and their empty membranes (i.e., ghosts). High-quality, label- and fixation-free visualization of hemoglobin was achieved at excitation wavelength 730 nm by detecting visible autofluorescence. Localization in the suspension and spatial distribution (i.e., mapping) of residual hemoglobin in erythrocyte ghosts has been resolved by 2PE. Prior to the 2PE mapping, the presence of residual hemoglobin in the bulk suspension of erythrocyte ghosts was confirmed by cyanmethemoglobin assay. 2PE analysis revealed that the distribution of hemoglobin in intact erythrocytes follows the cells' shape. Two types of erythrocytes, human and porcine, characterized with discocyte and echinocyte morphology, respectively, showed significant differences in hemoglobin distribution. The 2PE images have revealed that despite an extensive washing out procedure after gradual hypotonic hemolysis, a certain amount of hemoglobin localized on the intracellular side always remains bound to the membrane and cannot be eliminated. The obtained results open the possibility to use 2PE microscopy to examine hemoglobin distribution in erythrocytes and estimate the purity level of erythrocyte ghosts in biotechnological processes. [DOI: 10.1117/1.JBO.22.2.026003]

Keywords: multiphoton fluorescence microscopy; ultrafast lasers; hemoglobin; label-free imaging; erythrocytes; erythrocyte ghosts.
Paper 160493RR received Jul. 14, 2016; accepted for publication Jan. 24, 2017; published online Feb. 9, 2017.

1 Introduction

Two photon excitation fluorescence (2PE) microscopy as an advanced technique offers the possibility for noninvasive, label-free high resolution imaging of living cells and deep tissues by using the fluorescence emission from the endogenous fluorescent molecules.[1–3] The near-infrared radiation generates 2PE signals of endogenous fluorophores, such as tryptophan, riboflavines, nicotinamides, collagen, elastin, and so on, and thus provides rich morphological and biochemical information of biological systems.[4–6] Less investigated and reported is the intrinsic fluorescence of hemoglobin, the main intracellular component of erythrocytes, which emits a strong Soret fluorescence with the peak at 438 nm upon two-photon excitation by femtosecond pulses in red and near-infrared region (600 to 750 nm).[7,8] Such optical properties of hemoglobin opened the possibility to use 2PE microscopy as a tool for label-free imaging of erythrocytes, even *in vivo*.[9]

In addition to the well-known physiological functions of erythrocytes, they serve as a natural blood compartment participating at the same time in biodistribution, metabolism, and action of certain drugs.[10] Furthermore, intentional usage of human and animal erythrocytes, erythrocyte membranes (i.e., ghosts), and their nanoderivatives presents modern approach in terms of prolonged and controlled drug delivery systems.[11–14] Recently, we have reported the production of drug encapsulated porcine and bovine erythrocyte ghosts by gradual hypotonic hemolysis in much higher quantities than those described in literature so far.[13] However, it was noted that after the hemolysis process a certain amount of hemoglobin remains in the final suspension of the resulting erythrocyte ghosts.[13] The fraction of this so called residual hemoglobin, which cannot be easily eliminated from the system, significantly affects subsequent encapsulation processes and encapsulated drug releasing profile.[15] Although this residual hemoglobin can be determined by the spectrophotometric method (e.g., cyanmethemoglobin method), data on spatial distribution of hemoglobin at the single cell level in erythrocytes and remaining erythrocytes ghosts are scarce. Demonstrated spatial redistribution of hemoglobin throughout intact erythrocytes in patients with vascular disorders[16] promotes the importance of this parameter monitoring in disease diagnosis as well.

Based on the aforementioned wide applicability of erythrocytes in biomedical research and diagnostic tests, it is important to have a reliable microscopy method for single cell analysis, including spatial distribution of hemoglobin. Although phase contrast microscopy traditionally represents a fast method for tracking changes of erythrocytes during the gradual hypotonic hemolysis and appearance of erythrocyte ghosts,[17,13,18] it does not provide enough information for detailed morphological analysis. Unlike the phase contrast microscopy that visualizes

*Address all correspondence to: Aleksandar J. Krmpot, E-mail: krmpot@ipb.ac.rs

1083-3668/2016/$25.00 © 2016 SPIE

all the changes of the index of refraction regardless of their origin, 2PE microscopy has high chemical selectivity, thus enabling the visualization of the distribution of certain chemical compounds. Confocal microscopy, scanning electron microscopy, transmission electron microscopy, and atomic force microscopy are considered as the most powerful tools for structural analysis of various cells, including erythrocytes. However, these methods mandatorily include cell fixation and/or labeling which might influence the fragile cell structure.[19] So far, large numbers of optical microscopic techniques have been utilized for erythrocyte imaging. Comparative study of stained cells by confocal and unstained cells by holographic microscopy has been elaborated as shown in the work of Rappaz et al.[20] Scanning microphotolysis (Scamp), also referred to as fluorescence recovery after photobleaching, has been employed for erythrocyte examination either in a linear[21] or in a two photon, i.e., nonlinear, regime.[22] Volumetric imaging of erythrocytes using photoacoustic microscopy has been described by Shelton et al.,[23] while the same method in combination with confocal microscopy is used for hemoglobin oxygen saturation measurements., as shown by Wang et al.[24] 2PE was combined with stimulated Raman scattering for hemoglobin imaging in mouse retina.[25] Even second harmonic generation (SHG) microscopy, usually accompanied with 2PE as another modality of nonlinear microscopy, has been utilized for label free imaging of human erythrocytes membrane exposed to various glucose concentrations in phosphate buffered saline (PBS).[26] In addition to demonstration of the imaging possibilities of hemoglobin by the aforementioned techniques, 2PE has recently been applied in examination of particular biomedical problems related to erythrocytes: tracking blood vessels within the tissues[27] and photophysical characterization of sickle cell disease hemoglobin.[28]

In this work, we report label-free imaging of two kinds of erythrocytes, porcine and outdated human ones, at single cell level by 2PE microscopy, with the specific aim of investigating the spatial distribution (i.e., for mapping) of hemoglobin within intact erythrocytes and residual hemoglobin in erythrocyte membranes obtained after a gradual hypotonic hemolysis process. Furthermore, the quantity of residual hemoglobin was determined by analysis of 2PE images relative to the hemoglobin concentration in intact erythrocytes. This investigation opens the possibility to use 2PE microscopy as a tool for quality assessment of erythrocytes and erythrocyte membranes as a starting material in various biotechnological processes, such as the production of erythrocyte-based drug delivery systems[13,15] or isolation of hemoglobin.[18,29] Additionally, 2PE microscopy could help in revealing the ability of erythrocyte membranes, originating from different species, to bind different amounts of hemoglobin. Since various processes require various levels of purity, this information is important for the selection of raw material.

2 Materials and Methods

2.1 *Blood Samples*

Porcine slaughterhouse blood and human outdated blood were used as starting biological materials. Porcine blood was taken from the jugular veins of Swedish Landrace swine and collected in a sterile glass bottle with 3.8% sodium-citrate as an anticoagulant, at slaughterhouse "PKB Imes" in Belgrade, Serbia. Blood samples were transported at ambient temperature and processing started 2 h after the collection. The outdated human erythrocyte concentrates were from the Institute for Transfusiology and Hemobiology, Military Medical Academy, Belgrade, Serbia. The erythrocytes were enriched by the standard procedure and preserved in saline-adenine-glucose-mannitol solution (each 100 mL contains 0.900 g dextrose monohydrate, 0.877 g sodium chloride, 0.0169 g adenine, and 0.525 g mannitol) for 42 days at 4°C. The outdated cell packs were anonymized prior to distribution, and the link to the donor was broken. If not used for the research, the cell packs would have been discarded.

2.2 *Preparation of Erythrocytes and Erythrocyte Membranes (i.e., Ghosts)*

Both porcine and human erythrocytes were precipitated by blood centrifugation at $2450 \times g$ for 20 min at 4°C. The plasma and leucocytes were carefully discarded by vacuum aspiration. The precipitated erythrocytes were resuspended in isotonic saline solution (0.9% NaCl), washed twice by centrifugation, and finally resuspended in an isotonic PBS, pH 7.2 to 7.4 (0.8% saline buffered with 10 mM sodium phosphate). Porcine and human erythrocyte ghosts were prepared by gradual hypotonic hemolysis[13,29] by using hypotonic 35-mM sodium phosphate/NaCl buffer for porcine and 5-mM sodium phosphate buffer for human erythrocytes (30 min, flow rate 150 mL/h.) After the hemolysis, the erythrocyte ghosts were precipitated by 40 min centrifugation at $3220 \times g$, at 4°C. Erythrocyte ghosts were washed out three times in the buffer solution used for hemolysis and finally in PBS solution. Concentration of hemoglobin in suspensions of erythrocytes and residual hemoglobin in erythrocyte ghosts were determined by the cyanmethemoglobin method.[30] To quantify residual hemoglobin, prior to the determination of the concentration, erythrocyte ghosts were dispersed in 1 mL of isotonic PBS containing 1% w/w of Triton X100 detergent.

2.3 *Experimental Setup for 2PE*

The homemade two-photon microscopy experimental setup is similar to that reported in our previous study.[31] The schematic of the setup is given in Fig. 1. The train of the femtosecond

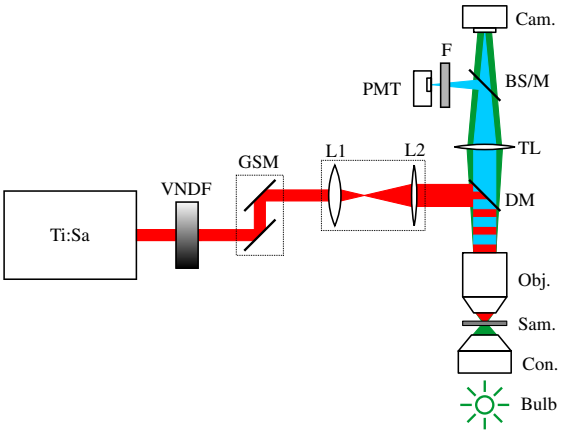

Fig. 1 Schematic of the imaging system: Ti:Sa, Ti:Sapphire laser, VNDF, variable neutral density filters, GSM, galvo scanning mirrors, L1 and L2, lenses, DM, dichroic mirror (short pass), Obj., microscope objective, Sam., sample, Con., condenser, Bulb, bulb for bright-field imaging illumination, TL, tube lens, BS/M, beam splitter or mirror, Cam., camera, F, filter, PMT, photomultiplier tube.

pulses is generated by the Ti:Sapphire laser (Coherent, Mira 900-F). The repetition rate is 76 MHz, and pulse duration is 160 fs. The galvoscanning mirrors (Cambridge Technologies, 6215H) are used to raster-scan the samples.

The laser beam is expanded in order to fill the entrance pupil of an objective (Carl Zeiss, EC Plan-NEOFLUAR, $40\times/1.3$ oil). A short-pass dichroic mirror (Thorlabs, M254H45) reflects the laser beam toward the objective, and transmits the signal toward the camera (Canon, EOS 50D) and the photomultiplier tube (PMT) (RCA, PF1006). The tube lens forms the sample image on the camera and/or PMT. The camera is used to take the bright-field image of the samples (green light in Fig. 1). The high intensity fluorescence can be seen by camera (blue light in Fig. 1). The commercial cameras usually have an infrared blocking filter. We removed this filter from our camera in order to see the backscattering/backreflection of the laser spot from the sample/cover slip which facilitated the alignment of the system. This is possible due to the fact that a small portion of the laser light leaks through the dichroic mirror (leakage of the laser is not shown in Fig. 1). A drawback of the infrared filter removing is the false coloring of the bright-field images. Thus, our bright-field images are greenish.

A beam-splitter or the mirror is used to reflect part of the signal or the complete signal to the PMT. An interference filter in front of the PMT removes scattered laser light. This filter is transparent for visible (415 to 685 nm) light, while blocking the IR and UV. Since the excitation wavelength is chosen in such a way that fluorescent signal comes predominantly from hemoglobin (Soret fluorescence), using the broadband filter ensures that all the fluorescent light will be collected, even from the wings of the fluorescent spectrum which is important in the case of relatively low excitation efficiency (see Sec. 2.4). This provides good signal-to-noise ratio and high contrast of images. Erythrocytes (hematocrit 5%, i.e., 5% suspension) and ghosts in the amount of 20 μL were allowed to settle onto a microscopic slide. Afterward, coverslips were put above settled cells and fixed to microscope slides. Imaging of erythrocytes and erythrocyte ghosts was performed at 730-nm excitation wavelength.

2.4 *Excitation Wavelength*

The excitation wavelength is of the great importance in this study and it has to be carefully selected according to its availability and the properties of the samples. Selection of the wavelength can significantly affect the chemical selectivity of the imaging, providing excitation of the specific and desired objects, and quality of the images by means of excitation efficiency and fluorescence strength. The excitation wavelength in this study is selected to be 730 nm by the following criteria:

- We have tested different excitation wavelengths within a Ti:Sapphire laser tuning range (700 to 1000 nm). Our excitation spectrum is consistent with the spectrum shown in study of Zheng et al.,[7] i.e., the excitation is the most efficient for the shortest wavelengths.
- The 2PE signal from hemoglobin at 650-nm excitation wavelength is reported to be more efficient[7] but we were not able to utilize shorter wavelengths than 700 nm due to the laser tuning range (700 to 1000 nm). Also, there is a significant leakage of the laser light to the PMT for wavelengths shorter than 730 nm. The cut-off wavelength of the dichroic mirror (hot mirror M254H45, Thorlabs, Inc.) is (700 ± 10) nm with transmission >97% for wavelengths longer than 710 nm, whereas full width at half maximum of the laser line is ~12 nm.
- The 2PE signal from glass (coverslips and microscope slides) is pronounced for wavelengths shorter than 730 nm. Thus, 730 nm is the shortest possible choice for the excitation wavelength to produce still high quality images.

3 Results and Discussion

In this study, erythrocyte membranes (ghosts) were prepared by gradual hypotonic hemolysis starting from slaughterhouse porcine and outdated human erythrocytes. During the process of gradual decrease of ionic strength of the solution surrounding erythrocytes, they swell and hemoglobin molecules leak out, leaving intact erythrocyte membranes.[13,17,18,29] Preparation of ghosts was followed by an extensive washing out procedure (to remove extracellular hemoglobin released from lysed erythrocytes). However, a small amount of hemoglobin, so called residual hemoglobin, always remains bound to membranes in resulting erythrocyte ghosts.[13]

Here, 2PE microscopy was used to quantify the relative decrease in hemoglobin's content at the end of the applied process of hemolysis and reveal its localization in the examined samples. All 2PE images are of the high quality by means of good signal-to-noise ratio, high visibility (contrast), high pixel resolution, and without or with minimal postmeasurement processing.

Bright-field microscopy images and corresponding autofluorescence 2PE images of starting porcine and human erythrocytes are presented in Figs. 2 and 3, respectively. 2PE images are acquired in 1024×1024 pixels resolution upon 30 times averaging of raw fluorescence signal. Intensity of pseudo-red color corresponds to the 2PE signal intensity.

According to image dimensions (30×30 μm^2) and physical resolution of our experiment, which is limited by diffraction and measured to be ~300 nm,[31] the minimal pixel resolution for faithful imaging of the object is set by Nyquist criterion to 200×200 pixels. In our case, 1024×1024 pixel resolution ensures that we overfill the Nyquist criterion and contribute to the high quality of the images.

As evident from Figs. 2(b) and 3(b), it is possible to notice localization of hemoglobin's content even from suspensions of

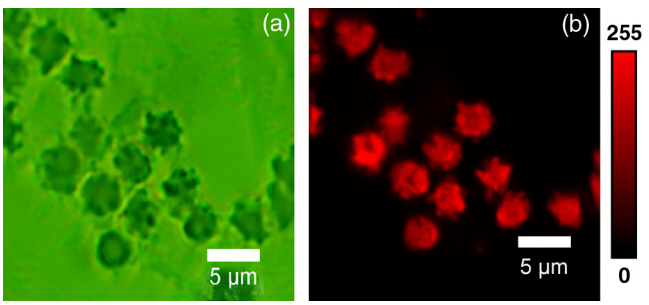

Fig. 2 Suspension of porcine erythrocytes: (a) bright-field microscopy image, (b) corresponding 2PE image revealing localization of hemoglobin; black, the lowest 2PE signal, red, the highest 2PE signal. 3-D model of examined human erythrocytes. (Video 1. MPEG, 6.16 MB [URL: http://dx.doi.org/10.1117/1.JBO.22.2.026003.1]).

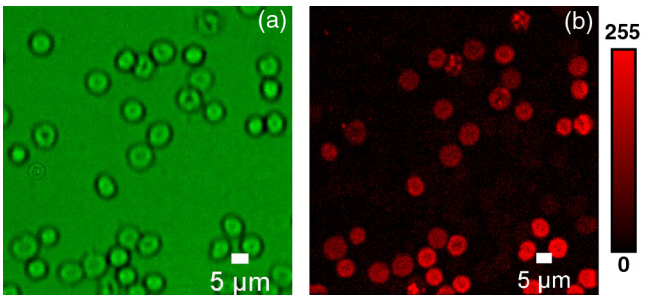

Fig. 3 Suspension of human erythrocytes: (a) bright-field microscopy image, (b) corresponding 2PE image revealing localization of hemoglobin; black, the lowest 2PE signal, red, the highest 2PE signal. Note that field of view (scale bar) is different than in a Fig. 2. It was changed because the region of interest was wider.

erythrocytes. Also, a 3-D model of examined human erythrocytes is displayed in Video 1.

Due to the presence of erythrocytes' methemoglobinreductase, hemoglobin in blood is predominately in its native ferrous form[32] which is desirable for the 2PE signal measurement. 2PE images and examination of hemoglobin distribution in a single erythrocyte for both examined types are given in Fig. 4. This result demonstrates that the resolution of the 2PE microscopy is good enough for the analysis of erythrocytes at the single cell level. As with the images in Fig. 3, these 2PE images are the results of averaging 30 individual images. Pseudocoloring corresponds to the 2PE signal intensity. No further processing of the image was performed, the data points in graphs represent the raw 2PE signal levels.

Based on the results in Fig. 4, we have confirmed that human erythrocytes have the normal morphology of biconcave discocytes,[33] whereas porcine erythrocytes have an echinocyte morphology. Such morphology of porcine erythrocytes is not a sign

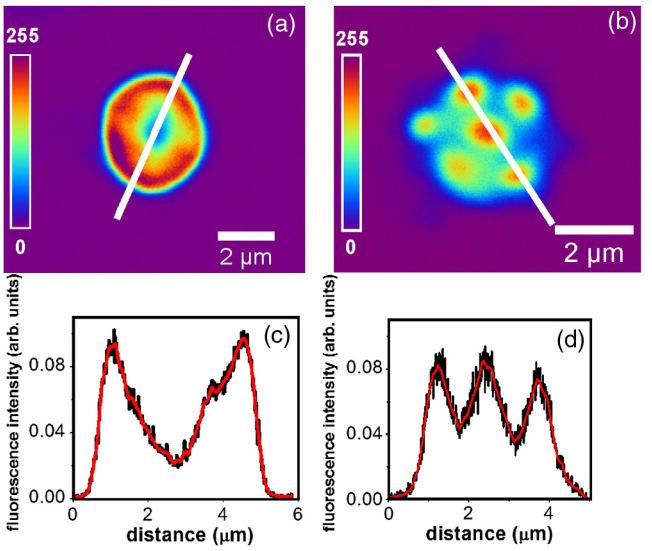

Fig. 4 Representative raw 2PE image of (a) human and (b) porcine erythrocyte. 2PE signal is presented in pseudocolor. Distribution of 2PE signals, i.e., hemoglobin concentration through the diameter of (c) human and (d) porcine erythrocyte. Black curves are raw data plot, red curves are obtained upon adjacent points averaging. Note that the two images are not recorded under the same experimental conditions; the intensities are not mutually normalized, thus they cannot be compared.

of some pathological condition but represents a common artifact in handling of porcine blood.[34]

Hemoglobin, which is the dominant component of erythrocytes, follows the cells' shape which can be easily observed by comparing the bright field and 2PE images. For human erythrocytes, its lowest density is observed to be in the central area [Fig. 4(a)], and in peripheral parts, its distribution was homogeneous. This finding is in agreement with the reported spatial distribution of hemoglobin in healthy human erythrocytes examined by confocal Raman spectroscopy[35] and atomic force microscopy.[36] On the other hand, for porcine erythrocytes, 2PE revealed a significant accumulation of hemoglobin in cells' protrusions. As shown in the study by Parshina et al.,[36] amphibian (frog) nucleated and mammalian (rat) nonnucleated healthy erythrocytes have a homogeneous distribution of cytosolic hemoglobin. Our results indicate that the deviations from the biconcave morphology of porcine erythrocytes probably affect the distribution of hemoglobin and lead to its accumulation in the cell protrusions. Taking into account that various pathological conditions are accompanied by uneven distribution of hemoglobin,[16,37] the developed method might be useful in their diagnosis. Until now it was described that isolated sickle cell disease hemoglobin (HbS) and malaria-infected red blood cells could be analyzed and photophysically characterized by multiphoton microscopy.[28,38]

The overall presence of residual hemoglobin in the final suspensions of erythrocyte ghosts was primarily determined by cyanmethemoglobin assay (Fig. 5). The concentration of residual hemoglobin was 7.21 and 1.76 g/L for the porcine and human samples, respectively. This reflects the decrease in concentrations of hemoglobin by 95% and 99% in the suspension of erythrocyte ghosts compared to the starting suspensions of porcine and outdated human erythrocytes, respectively. These amounts of residual hemoglobin in erythrocyte ghosts are consistent with the range reported in other studies.[39,40] However, the localization of residual hemoglobin in the suspension still remains unknown.

In addition to the spatial distribution of hemoglobin in intact human and porcine erythrocytes, images of residual hemoglobin in erythrocyte ghosts also can be obtained by 2PE (Figs. 6 and 7, respectively). The intensity of the 2PE signal depends on the concentration of the hemoglobin, but also on the pulse peak power, pulse duration, repetition rate, focal volume, excitation wavelength, etc. It is a nontrivial and time consuming task to quantify the dependence of the 2PE signal on hemoglobin concentration. In other words, it is almost impossible to determine

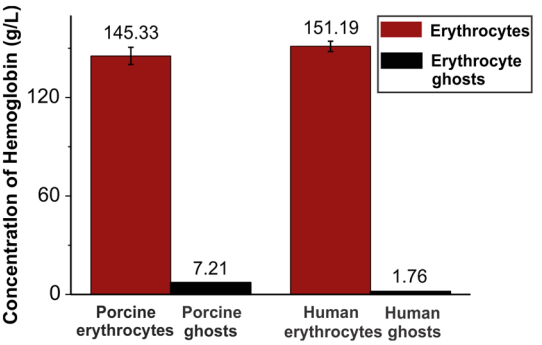

Fig. 5 Concentration of hemoglobin in erythrocytes and their ghosts obtained by gradual hemolysis. The concentration was determined by spectrophotometric cyanmethemoglobin method.

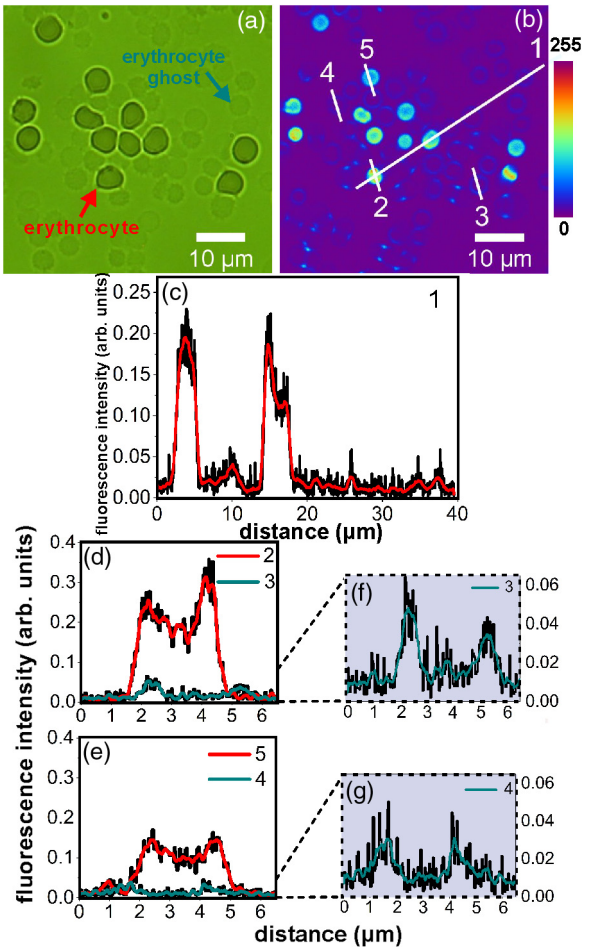

Fig. 6 Mixed suspension of human erythrocytes and resulting erythrocyte ghosts: (a) bright-field microscopy image; (b) 2PE image; (c–g) 2PE signal profiles along the corresponding lines at (b) image. Profiles 3 and 4 are given in magnified vertical scale in (f) and (g) graphs. Black curves are raw data plot, red and green curves are obtained upon adjacent points averaging.

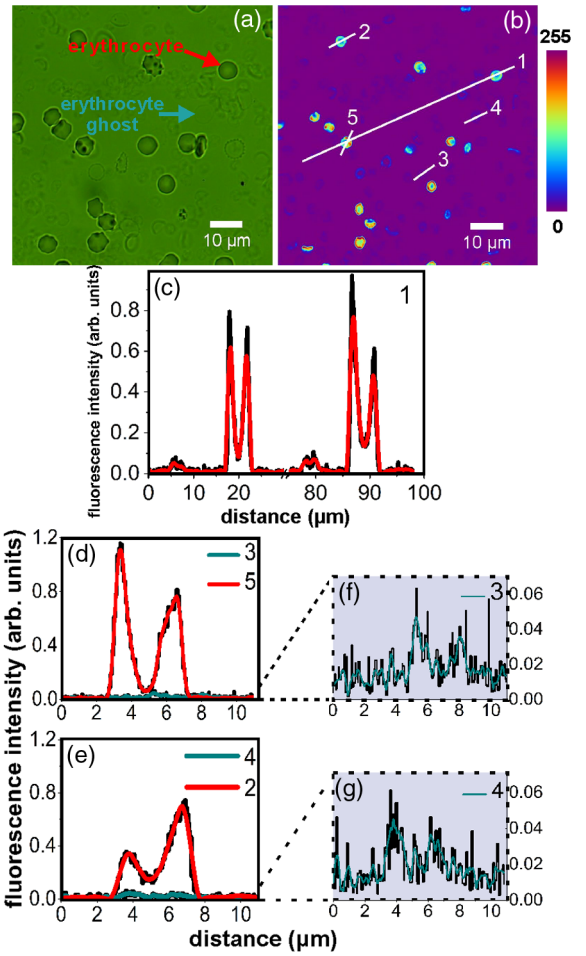

Fig. 7 Mixed suspension of porcine erythrocytes and resulting erythrocyte ghosts: (a) bright-field microscopy image; (b) 2PE image; (c–g) 2PE signal profiles along the corresponding lines at (b) image. Profiles 3 and 4 are given in magnified vertical scale in (f) and (g) graphs. Black curves are raw data plot, red and green curves are obtained upon adjacent points averaging.

absolute concentration from the 2PE signal since one has to keep all other parameters constant in separate measurements. In order to evaluate the local change (i.e., decrease) in hemoglobin content after the hemolysis, we mixed the ghosts with intact erythrocytes. In this way, we can evaluate the local content of hemoglobin, i.e., distribution of hemoglobin across erythrocytes and ghosts, and not just an average value for a whole cell or suspension. From the image data we obtained, the variation of intensity along appropriately chosen representative lines is shown in Figs. 6(b) and 7(b). The line is chosen in a way to intercept at least two erythrocytes and two ghosts which provide up to eight representative points positioned in the proximity of the membrane within the cells for comparison of 2PE signals. Note that the signals from the chosen points provide highly localized data for the comparison, opposite to the cyanmethemoglobin assay, which is intrinsically an averaging method. This ensures the same excitation parameters for both erythrocytes and erythrocyte ghosts. The above procedure ensures that the peak ratio from the 2PE intensity profile is equal to the concentration ratio in the untreated erythrocyte(s) and the ghost(s). We emphasize that this simple step enables us to determine changes in the content of residual hemoglobin in ghosts relative to the starting content of hemoglobin in intact erythrocytes, but not the absolute concentration.

There is no significant autofluorescence signal upon two photon excitation at 730 nm from any other common molecular species that can be found in erythrocytes and which could significantly affect the obtained results, except hemoglobin. Namely, lipids and saccharides are essentially nonfluorescent,[41] while aromatic amino acids as constituents of proteins, such tryptophan, phenylalanine, and tyrosine, have an absorption maximum of 280 nm[41] and cannot contribute significantly to autofluorescence generated by two-photon excitation at 730 nm. Pyridine nucleotides NADH and NADPH have an absorption maximum of 340 nm[42] and FAD has two excitation maxima at 360 and 450 nm. According to their excitation maximum, they could contribute the autofluorescence generated by two-photon excitation at 730 nm. However, their molar ratios to hemoglobin within erythrocytes (calculated based on data given in several studies)[43–45] are completely negligible.

As can be seen from Figs. 6 and 7, after the conversion of erythrocytes to empty erythrocyte membranes, fluorescence emission from hemoglobin significantly decreased, but was still detectable. Therefore, the applied process that we used allows the production of ghosts; however, a certain amount

of the hemoglobin always remains bound to the membrane. Comparing the peak values from Figs. 6(d) and 6(e) (red curves) to those in Figs. 6(f) and 6(g), one can estimate lower fluorescence emissions for both porcine and human erythrocyte ghosts in comparison to respective erythrocytes. Our results suggest that residual hemoglobin in the suspension was localized on the intracellular side of the ghost membranes. The 2PE signal in the internal volume of both, human and porcine erythrocyte ghosts, is at the noise level, thus hemoglobin content is negligible.

These results support already reported data on hemoglobin's ability to bind to erythrocyte membranes via a transmembrane protein, e.g., band 3[46] or some other cytoskeleton proteins via α globin chains.[47] This phenomenon that we have confirmed by 2PE microscopy could be used as a valuable marker of inevitable oxidative damages[48] emerged during *in vitro* storage and erythrocytes handling. The higher concentration of residual hemoglobin obtained in porcine ghosts relative to initial concentration can be explained by specific membrane lipid composition and their high susceptibility to oxidative stress induced by reactive oxygen species[49] related to a lower level of enzymes protectants against oxidative damages.[50]

Erythrocyte ghosts are extensively studied systems and have numerous potential applications. In addition to their usage as controlled drug delivery systems, they represent one of the most promising *in vitro* systems for drug partitioning studies and determination of the drug partition coefficient Kps.[51] In food science they are used for an estimation of antioxidant activity of different nutritional compounds.[52,53] Erythrocyte ghosts are suitable models for investigating membrane transport phenomena,[54] glucose translocation through biological membranes,[55] uptake and metabolism of different compounds,[56] etc. It is interesting to note that despite their widespread application, there are no studies estimating residual hemoglobin although it may significantly affect the quality of the final product. Apart from the mentioned study that suggests a positive correlation between the total content of membrane-bound hemoglobin and the level of oxidant stress,[48] it has been shown that iron from membrane-bound hemoglobin catalyzes the formation of reactive oxygen species which attack the cell membrane. This leads to peroxidation of membrane unsaturated lipids and disturbed structure and function of the membrane[57] and may directly affect the quality of the final product and/or obtained results.

In addition to using 2PE microscopy for analysis of erythrocyte ghosts as in the mentioned model or drug delivery systems, the results of this study also open a possibility of using 2PE microscopy in analysis of the spatial distribution of hemoglobin in erythrocytes in different physiological and pathological conditions. The spatial distribution of hemoglobin within erythrocytes can give information of the oxygen-transport capability and help by providing accurate diagnosis and appropriate treatment in erythrocytes disorders both in humans and animals.

4 Conclusion

In this study, we have demonstrated that 2PE microscopy can be used in analysis of the spatial distribution of hemoglobin in erythrocytes and erythrocyte ghosts, at an individual cell level. Although the maximal excitation efficiency for hemoglobin is at shorter wavelengths, high quality images can still be obtained using femtosecond pulses at 730 nm directly from a Ti:Sa oscillator. As opposed to the common spectroscopic methods such as cyanmethemoglobin assay that is intrinsically averaging, providing results for hemoglobin concentration drop after the hemolysis process in the bulk sample, 2PE microscopy gives results on hemoglobin localization and its fluorescence intensity change in randomly chosen points within the ghost-erythrocytes sample. Obtained results suggest that residual hemoglobin in erythrocyte ghosts, either human or porcine ones, is located mainly near the cell membrane rather than uniformly distributed. In addition, 2PE microscopy enables imaging of the distribution of hemoglobin in the protrusions of erythrocytes with morphology of echinocytes, thus it can be used for mapping of hemoglobin in erythrocytes morphologically different from the normal discocytes.

High-quality, label- and fixation-free visualization of hemoglobin can be achieved at 730-nm excitation wavelength. The 2PE fluorescence signal from residual hemoglobin at representative points near the cell membrane in the ghosts was reported to have lower intensity than at the corresponding points in intact erythrocytes. Obtained results suggest that residual hemoglobin in erythrocyte ghosts is located mainly near the cell membrane rather than uniformly distributed.

In such a way, through an application of 2PE microscopy hemoglobin distribution in erythrocytes together with residual hemoglobin content and distribution in the resulting erythrocyte ghosts can be directly and relatively easily estimated. The proposed method could be of significant importance for identifying different pathological or nonpathological conditions and application in material selection in biotechnological processes.

Disclosures

The authors declare no conflicts of interest.

Acknowledgments

This work has been supported by Ministry of Education, Science and Technological Development of the Republic of Serbia (Project Nos. III 46010, OI 171005, OI 171038, and III45016) and by the project NPRP 6-021-1-005 from the Qatar National Research Fund (member of the Qatar Foundation).

References

1. K. König et al., "Multiplex FISH and three-dimensional DNA imaging with near infrared femtosecond laser pulses," *Histochem. Cell Biol.* **114**(4), 337–345 (2000).
2. R. Weigert et al., "Intravital microscopy: a novel tool to study cell biology in living animals," *Histochem. Cell. Biol.* **133**(5), 481–491 (2010).
3. B. R. Masters and P. So, *Handbook of Biomedical Nonlinear Optical Microscopy*, Oxford University Press, New York (2008).
4. H. Kolesová et al., "Comparison of different tissue clearing methods and 3D imaging techniques for visualization of GFP-expressing mouse embryos and embryonic hearts," *Histochem. Cell. Biol.* **146**, 141–152 (2016).
5. L. Peralta et al., "In vivo evaluation of cervical stiffness evolution during induced ripening using shear wave elastography, histology and 2 photon excitation microscopy: insight from an animal model," *PloS One* **10**, e0133377 (2015).
6. B. G. Wang et al., "Intraocular multiphoton microscopy with subcellular spatial resolution by infrared femtosecond lasers," *Histochem. Cell Biol.* **126**(4), 507–515 (2006).
7. W. Zheng et al., "Two-photon excited hemoglobin fluorescence," *Biomed. Opt. Express* **2**, 71–79 (2010).
8. G. O. Clay, C. B. Chaffer, and D. Kleinfeld, "Large two-photon absorptivity of hemoglobin in the infrared range of 780-880 nm," *J. Chem. Phys.* **126**, 025102 (2007).

9. D. Li et al., "Time-resolved detection enables standard two-photon fluorescence microscopy for *in vivo* label-free imaging of microvasculature in tissue," *Opt. Lett.* **36**(14), 2638–2640 (2011).
10. P. H. Hinderling, "Red blood cells: a neglected compartment in pharmacokinetics and pharmacodynamics," *Pharmacol. Rev.* **49**(3), 279–295 (1997).
11. V. Leuzzi et al., "Erythrocyte-mediated delivery of recombinant enzymes," *Inherit Metab. Dis.* **39** (4), 519–530 (2016).
12. V. Bourgeaux et al., "Drug-loaded erythrocytes: on the road toward marketing approval," *Drug Des. Dev. Ther.* **10**, 665–676 (2016).
13. I. Kostić et al., "Erythrocyte membranes from slaughterhouse blood as potential drug vehicles: isolation by gradual hypotonic hemolysis and biochemical and morphological characterization," *Colloids Surf. B* **122**, 250–259 (2014).
14. R. Deak et al., "Physicochemical characterization of artificial nanoerythrosomes derived from erythrocyte ghost membranes," *Colloids Surf. B* **135**, 225–234 (2015).
15. I. T. Drvenica et al., "Biomembranes from slaughterhouse blood erythrocytes as prolonged release systems for dexamethasone sodium phosphate," *Biotechnol. Prog.* **32**, 1046–1055 (2016).
16. V. V. Revin et al., "Study of the structure, oxygen-transporting functions, and ionic composition of erythrocytes at vascular diseases," *Biomed. Res. Int.* **2015**, 973973 (2015).
17. D. Danon, "Osmotic hemolysis by a gradual decrease in the ionic strength of the surrounding medium," *J. Cell. Comp. Physiol.* **57**, 111–117 (1961).
18. R. Stojanović et al., "Isolation of hemoglobin from bovine erythrocytes by controlled hemolysis in the membrane bioreactor," *Appl. Biochem. Biotechnol.* **166**, 1491–1506 (2012).
19. E. Wisse et al., "Fixation methods for electron microscopy of human and other liver," *World J. Gastroenterol.* **16**, 2851–2866 (2010).
20. B. Rappaz et al., "Comparative study of human erythrocytes by digital holographic microscopy, confocal microscopy, and impedance volume analyzer," *Citometry* **73A**, 895–903 (2008).
21. M. Tschödrich-Rotter et al., "Optical single-channel analysis of the aerolysin pore in erythrocyte membranes," *Biophys. J.* **70**, 723–732 (1996).
22. U. Kubitschek et al., "Two-photon scanning microphotolysis for three-dimensional data storage and biological transport measurements," *J. Microsc.* **182**, 225–233 (1996).
23. R. L. Shelton, S. P. Mattison, and B. E. Applegate, "Volumetric imaging of erythrocytes using label-free multiphotonphotoacoustic microscopy," *J. Biophotonics* **7**, 834–840 (2014).
24. Y. Wang et al., "In vivo integrated photoacoustic and confocal microscopy of hemoglobin oxygen saturation and oxygen partial pressure," *Opt. Lett.* **36**, 1029–1031 (2011).
25. S. He et al., "Label-free nonlinear optical imaging of mouse retina," *Biomed. Opt. Express* **6**, 1055–1066 (2015).
26. D. Lev et al., "d-Glucose-induced second harmonic generation response in human erythrocytes," *J. Phys. Chem.* **113**, 2513–2518 (2009).
27. N. L. Garrett et al., "Exploring uptake mechanisms of oral nanomedicines using multimodal nonlinear optical microscopy," *J. Biophotonics* **5**, 458–468 (2012).
28. G. D. Vigil and S. S. Howard, "Photophysical characterization of sickle cell disease hemoglobin by multi-photon microscopy," *Biomed. Opt. Express* **6**, 4098–4104 (2015).
29. B. Bugarski and N. Dovezenski, "Hemofarm Koncern. Verfahrenzur Herstellung von Hemoglobin," Deutsches Patentamt DE 19707508 (2000).
30. O. W. Van Assendelft, A. H. Holtz, and S. M. Lewis, *Recommended Method for the Determination of the Haemoglobin Content of Blood*, I. C. S. H. Publications, World Health Organization (1984).
31. M. D. Rabasović et al., "Nonlinear microscopy of chitin and chitinous structures: a case study of two cave-dwelling insects," *J. Biomed. Opt.* **20**(1), 016010 (2015).
32. A. Mansouri and A.A. Lurie, "Concise review: methemoglobinemia," *Am. J. Hematol.* **42**, 7–12 (1993).
33. M. Diez-Silva et al., "Suresh shape and biomechanical characteristics of human red blood cells in health and disease," *MRS Bull.* **35**(5), 382–388S (2010).
34. J. D. Weiss and K. J. Wardrop, Eds., *Schalm's Veterinary Haematology*, 6th ed., pp. 144–151, Blackwell Publishing Ltd., Ames (2010).
35. L. Kang et al., "Confocal Raman microscopy on single living young and old erythrocytes," *Biopolymers* **89**, 951–959 (2008).
36. E.Y. Parshina et al., "Combined Raman and atomic force microscopy study of hemoglobin distribution inside erythrocytes and nanoparticle localization on the erythrocyte surface," *Laser Phys. Lett.* **10**, 075607 (2013).
37. J. P. Greer et al., *Wintrobe's Clinical Hematology*, 13th ed., Lippincott Williams & Wilkins, Philadelphia (2014).
38. J. Mauritz et al., "Biophotonic techniques for the study of malaria-infected red blood cells," *Med. Biol. Eng. Comput.* **48**, 1055–1063 (2010).
39. S. S. Bernstein et al., "Method for the preparation of posthemolitic residue or stroma of erythrocytes," *J. Biol. Chem.* **122**, 507–514 (1938).
40. D. Danon, A. Nevo, and Y. Marikovsky, "Preparation of erythrocyte ghosts by gradual haemolysis in hypotonic aqueous solution," *Bull. Res. Counc. Israel* **6E**, 36 (1956).
41. J. R. Lakowicz, "Protein fluorescence," Chapter 16 in *Principles of Fluorescence Spectroscopy*, 3rd ed., J. R. Lakowicz, Ed., pp. 530–578, Springer US, New York (2006).
42. H. Andersson et al., "Autofluorescence of living cells," *J. Microsc.* **191**(Pt 1), 1–7 (1998).
43. Y. Ogasawara, M. Funakoshi, and K. Ishii, "Determinationof reduced nicotinamide adenine dinucleotide phosphate concentration using high-performance liquid chromatography with fluorescence detection: ratio of the reduced form as a biomarker of oxidative stress," *Biol. Pharm. Bull.* **32**(11), 1819–1823 (2009).
44. S. Hustad et al., "Riboflavin, flavin mononucleotide, and flavinadenine dinucleotide in human plasma and erythrocytes at baseline and afterlow-dose riboflavin supplementation," *Clin. Chem.* **48**(9), 1571–1577 (2002).
45. K. J. Smock and S. L. Perkins, "Examination of the blood and bone marrow," Chapter 1 in *Wintrobe's Clinical Hematology*, J. P. Greer et al., Eds., pp. 1–64, Lippincott Williams & Wilkins, Philadelphia (2014).
46. J. Eisinger, J. Flores, and J. M. Salhany, "Association of cytosol hemoglobin with the membrane in intact erythrocytes," *Proc. Natl. Acad. Sci. U. S. A.* **79**, 408–412 (1982).
47. K. Murakami and S. Mawatari, "Oxidation of hemoglobin to methemoglobin in intact erythrocyte by a hydroperoxide induces formation of glutathionylhemoglobin and binding of alpha-hemoglobin to membrane," *Arch. Biochem. Biophys.* **417**(2), 244–250 (2003).
48. R. Sharma and B. R. Premachandra, "Membrane-bound hemoglobin as a marker of oxidative injury in adult and neonatal red blood cells," *Biochem. Med. Metab. Biol.* **46**(1), 33–44 (1991).
49. E. Brzezińska-Slebodzińska, "Species differences in the susceptibility of erythrocytes exposed to free radicals in vitro," *Vet. Res. Commun.* **27**(3), 211–217 (2003).
50. J. K. Vodela and R. R. Dalvi, "Erythrocyte glutathione-S-transferase activity in animal species," *Vet. Hum. Toxicol.* **39**, 9–11 (1997).
51. A. A. Omran, "An in vitro spectrometric method for determining the partition coefficients of non-steroidal anti-inflammatory drugs into human erythrocyte ghost membranes," *Spectrochim. Acta. A* **104**, 461–467 (2013).
52. S. Kumazawa et al., "Antioxidant activity of polyphenols in carob pods," *J. Agric. Food Chem.* **50**, 373–377 (2002).
53. S. Chaudhuri et al., "Interaction of flavonoids with red blood cell membrane lipids and proteins: antioxidant and antihemolytic effects," *Int. J. Biol. Macromol.* **41**, 42–48 (2007).
54. U. Kubitschek et al., "Two-photon scanning microphotolysis for three-dimensional data storage and biological transport measurements," *J. Microsc.* **182**, 225–233 (1996).
55. R. D. Taverna and R. G. Langdon, "Reversible association of cytochalasin B with the human erythrocyte membrane. Inhibition of glucose transport and the stoichiometry of cytochalasin binding," *Biochim. Biophys. Acta* **323**, 207–219 (1973).
56. J. Schrader, R. M. Berne, and R. Rubio, "Uptake and metabolism of adenosine by human erythrocyte ghosts," *Am. J. Physiol.* **223**, 159–166 (1972).
57. A. W. Girotti and J. P. Thomas, "Damaging effects of oxygen radicals on resealed erythrocyte ghosts," *J. Biol. Chem.* **3**, 1744–1752 (1984).

Katarina Bukara graduated from Faculty of Pharmacy, University of Belgrade. Currently, she is doing a joint PhD at University of Belgrade,

Serbia (biotechnology and biochemical engineering) and University of Antwerp, Belgium (pharmaceutical sciences). Her research concerns the development of controlled drug delivery systems for steroids and nonsteroidal anti-inflammatory drugs based on empty erythrocyte membranes and biodegradable polymers.

Svetlana Jovanić obtained her master's degee in biophysics at the University of Belgrade, Serbia. Currently, she is a junior research associate at the Institute of Physics in Belgrade and a member of the Laboratory for Biophotonics. Her PhD research is based on investigation of neurodegeneration disorders by usage of nonlinear laser scanning microscopy (two photon excitation fluorescence and second harmonic generation) on cells and tissues.

Ivana T. Drvenica is a research associate at Innovation Centre of Faculty of Technology and Metallurgy, University of Belgrade (TMF). She obtained her MSc degree in pharmaceutical sciences from the Faculty of Pharmacy, University of Belgrade, in 2009. In collaboration with Institute for Medical Research, University of Belgrade, she obtained her PhD in biotechnology at TMF in 2015 on development and characterization of erythrocyte membranes from wasted slaughterhouse blood as prolonged drug delivery vehicles.

Ana Stančić is a third-year PhD student at the Faculty of Biology, carrying out experiments for her thesis at the Institute for Medical Research, University of Belgrade. She is the stipendist of the Ministry of Education, Science and Technological Development of the Republic of Serbia. Her work is focused on *in vitro* testing of biological effects of empty erythrocyte membranes (i.e., ghosts), hemoglobin-based products and development of modern glucocorticoid derivatives.

Vesna Ilić is a molecular biologist and physiologist. She received her PhD in immunobiology. She is a head of the Group of Immunology, Institute for Medical Research, University of Belgrade. Her areas of interests include immunoglobulins and immune complexes, signaling in cells of immune and hematopoietic systems, biological effects of mesenchymal stem cells, systems for prolonged drug delivery based on erythrocytes, and heme iron formulations for prevention or treatment of anemia.

Mihailo D. Rabasović obtained his BS, MS, and PhD degrees from the physics department of the University of Belgrade in field of applied physics. His current research interests include photoacoustics, microscopy, and correlation spectroscopy. In the field of microscopy, he is interested in nonlinear and label-free techniques.

Dejan Pantelić is a research professor at the Institute of Physics in Belgrade, Serbia. His interests include holography, biophotonics, biomimetics, and microscopy. He has published more than 100 papers in refereed journals and conferences. He is a member of the Optical Society of America.

Branislav Jelenković is a research professor and head of the Photonic Center, Institute of Physics, University of Belgrade. He earned his bachelor's degree at Faculty of Electrical Engineering, University of Belgrade (1977) and PhD in physics at Faculty of physics, University of Belgrade (1985). He is a member of Serbian Academy of Science and Art, Optical Society of Serbia (copresident), American Optical Society. He won Institute of Physics Award in 2010. He has over 100 publications in peer-reviewed journals, with over 2500 citations.

Branko Bugarski obtained a PhD in 1992 at the University of Queens, Canada. Currently, he is a professor of chemical engineering at Faculty of Technology and Metallurgy, University of Belgrade, Serbia. During 1998, he was a guest professor at Oregon State University and Massachusetts Institute of Technology. The majority of his research interests are focused on immobilization, encapsulation, nanoparticles, and their application in medicine and pharmacy.

Aleksandar J. Krmpot, assistant research professor at the Institute of Physics Belgrade received his PhD in quantum optics from the University of Belgrade, Serbia. His research activities are in quantum optics (coherent optical effects) and biophotonics (microscopy and imaging). His current research activities are the development and application of nonlinear microscopy for bioimaging at Institute of Physics, Belgrade, Serbia and multifocal correlation microscopy for studies of molecular diffusion dynamics at Karolinska Institute, Stockholm, Sweden.